J|A|C|S
ARTICLES
Published on Web 06/19/2003

A DNA Aptamer as a New Target-Specific Chiral Selector for HPLC

Mickael Michaud, Eric Jourdan, Annick Villet, Anne Ravel, Catherine Grosset, and Eric Peyrin*

Contribution from the Equipe de Chimie Analytique, Département de Pharmacochimie Moléculaire (UMR 5063 CNRS-UJF), ICMG FR 2607, UFR de Pharmacie de Grenoble, Université Joseph Fourier, Avenue de Verdun, 38240 Meylan, France

Received February 4, 2003; E-mail: eric.peyrin@ujf-grenoble.fr

Abstract: In this paper, a DNA aptamer, known to bind stereospecifically the D-enantiomer of an oligopeptide, i.e., arginine-vasopressin, was immobilized on a chromatographic support. The influence of various parameters (such as column temperature, eluent pH, and salt concentration) on the L- and D-peptide retention was investigated in order to provide information about the binding mechanism and then to define the utilization conditions of the aptamer column. The results suggest that dehydration at the binding interface, charge−charge interactions, and adaptive conformational transitions contribute to the specific D-peptide-aptamer complex formation. A very significant enantioselectivity was obtained in the optimal binding conditions, the D-peptide being strongly retained by the column while the L-peptide eluted in the void volume. A rapid baseline separation of peptide enantiomers was also achieved by modulating the elution conditions. Furthermore, it was established that the aptamer column was stable during an extended period of time. This work indicates that DNA aptamers, specifically selected against an enantiomer, could soon become very attractive as new target-specific chiral selectors for HPLC.

Introduction

The separation of enantiomers is an area of increasing interest in pharmaceutical or biological fields, as two enantiomers of the same chiral molecule may have completely different physiological behaviors. For example, it is well established that, frequently, one of the two enantiomers of a drug is pharmaceutically active, while the other one can be inactive or toxic. Thus, the industrials are becoming more and more interested in new separation methodology for both analysis and purification of optical antipodes. Intensive research efforts are carried out for the discovery of new peptidic drugs.[1] Notably, important papers have focused on the usefulness of peptides composed of D-amino acids (D-peptides) for the development and identification of potential drugs with resistance to proteolytic degradation.[2] Therefore, several papers have been reported for the chiral separation of oligopeptides.[3] High-performance liquid chromatography (HPLC) is one of the most suitable techniques for enantiomeric resolution at analytical (or preparative) levels because of its high efficiency, speed, reproducibility, and wide range of applications. During the last two decades, various types of chiral selectors have been introduced as chiral stationary phases (CSPs) in HPLC. The chiral selectors commonly used for the production of CSPs are amino acids,[4] proteins,[5] crown-ethers,[6] oligo- and polysaccharides,[7] or more recently macrocyclic antibiotics.[8] However, the conventional chiral stationary phases are not specifically designed for the enantiomers to separate, making screening of stationary phase libraries a necessary step in the method development. Therefore, research efforts have been carried out in order to obtain tailor-made chiral selectors. Two major approaches have been reported involving

(1) (a) Boss, C.; Boli, M.; Weller, T. *Curr. Med. Chem*. **2002**, *9*, 349. (b) Yu, W.; Liang, Y.; Liu, K.; Zhao, Y.; Fei, G.; Wang, H. *J. Pept. Res*. **2002**, *59*, 134. (c) David, S. A. *J. Mol. Recognit*. **2001**, *14*, 370. (d) Beckers, T.; Bernd, M.; Kutscher, B.; Kuhne, R.; Hoffmann, S.; Reissmann, T. *Biochem. Biophys. Res. Commun*. **2001**, *289*, 653.

(2) (a) Zhou, N.; Luo, Z.; Luo, J.; Fan, X.; Cayabyab, M.; Hiraoka, M.; Liu, D.; Han, X.; Pesavento, J.; Dong, C. Z.; Wang, Y.; An, J.; Kaji, H.; Sodroski, J. G.; Huang, Z. *J. Biol. Chem*. **2002**, *277*, 17476. (b) Sia, S. K.; Kim, P. S. *Biochemistry* **2001**, *40*, 8981. (c) Eckert, D. M.; Malashkevich, V. N.; Hong, L. H.; Carr, P. A.; Kim, P. S. *Cell* **1999**, *99*, 103. (d) Hamy, F.; Felder, E. R.; Heizmann, G.; Lazdins, J.; Aboul-Ela, F.; Varani, G.; Karn, J.; Klimkait, T. *Proc. Natl. Acad. Sci. U.S.A.* **1997**, *94*, 3548. (e) Schumacher, T. N.; Mayr, L. M.; Minor, D. L.; Milhollen, M. A.; Burgess, M. W.; Kim, P. S. *Science* **1996**, *271*, 1854.

(3) (a) Czerwenka, C.; Lämmerhofer, M.; Maier, N. M.; Rissanen, K.; Lindner, W. *Anal. Chem*. **2002**, *74*, 5658. (b) Wan, H.; Blomberg, L. G. *J. Chromatogr. A* **2000**, *875*, 43. (c) Berthod, A.; Liu, Y.; Bagwill, C.; Armstrong, D. W. *J Chromatogr. A* **1996**, *731*, 123.

(4) (a) Gasparrini, F.; Misiti, D.; Still, W. C.; Villani, C.; Wennemers, H. *J. Org. Chem*. **1997**, *62*, 8221. (b) Pirkle, W. H.; Pochapsky, T. C. *J. Am. Chem. Soc*. **1986**, *108*, 352. (c) Pirkle, W. H.; Finn, J. M. *J. Org. Chem*. **1981**, *46*, 2935.

(5) (a) Hage, D. S. *J. Chromatogr. B* **2002**, *768*, 3. (b) Fornstedt, T.; Gotmar, G.; Andersson, M.; Guiochon, G. *J. Am. Chem. Soc*. **1999**, *121*, 1164. (c) Jacobson, S. C.; Golshan-Shirazi, S.; Guiochon, G. *J. Am. Chem. Soc*. **1990**, *112*, 6492. (d) Hermansson, J. *J. Chromatogr*. **1985**, *325*, 379.

(6) (a) Hilton, M.; Armstrong, D. W. *J. Liq. Chromatogr*. **1991**, *14*, 3673. (b) Dotsevi, G.; Sogaah, Y.; Cram, D. J. *J. Am. Chem. Soc*. **1975**, *97*, 1259.

(7) (a) Kubota, T.; Yamamoto, C.; Okamoto, Y. *J. Am. Chem. Soc*. **2000**, *122*, 4056. (b) Lipkowitz, K. B.; Pearl, G.; Coner, B.; Peterson, M. A. *J. Am. Chem. Soc*. **1997**, *119*, 600. (c) Berthod, A.; Chang, S. C.; Armstrong, D. W. *Anal. Chem*. **1992**, *64*, 395. (d) Okamoto, Y.; Kawashima, M.; Yamamoto, K.; Hatada, K. *Chem. Lett*. **1984**, *739*.

(8) (a) Slama, I.; Dufresne, C.; Jourdan, E.; Fahrat, F.; Villet, A.; Ravel, A.; Grosset, C.; Peyrin, E. *Anal. Chem*. **2002**, *74*, 5205. (b) Peter, A.; Torok, G.; Armstrong, D. W.; Toth, G.; Tourwé, D. *J. Chromatogr. A* **1998**, *828*, 177. (c) Armstrong, D. W.; Liu, Y.; Ekborg-Ott, K. H. *Chirality* **1995**, *7*, 474. (d) Armstrong, D. W.; Tang, Y.; Chen, S.; Zhou, Y.; Bagwill, C.; Chen, J. R. *Anal. Chem*. **1994**, *66*, 1473.

 10.1021/ja034483t CCC: $25.00

the production of imprinted polymers[9] or antibodies.[10] However, both these two tailor-made chiral stationary phases have some drawbacks. Columns packed with imprinted materials exhibit relatively reduced apparent enantioselectivity, peak asymmetry, and low sample load capacity due to a heterogeneous population of binding sites and a lack of recognition of a number of important compound classes.[9a,11] In addition, the use of antibodies as affinity stationary phases has constraints such as low surface loading, difficulty in tailoring the selectivity, and lack of antibodies for weakly immunogenic molecules.[12]

Nucleic acid aptamers are oligonucleotides, often single-stranded, with selective binding properties originating from in vitro selection experiments (SELEX methodology).[13] DNA or RNA aptamers have been identified for a broad spectrum of targets including metal ions,[14] organic dyes,[15] amino acids,[16] peptides,[17] proteins,[18] nucleotides,[19] and drugs.[20] The selectivity and affinity of aptamers have been recently used with much interest in flow cytometry,[21] sensors,[20a,22] ELISA-type assays,[23] capillary electrophoresis,[24] and affinity chromatography.[25] Aptamers present various advantages. They are produced by chemical synthesis in a short time, at low cost, with reproducibility and accuracy and at a high degree of purity. It is also easily possible to change their sequence in order to modulate their binding selectivity. In addition, they can be modified at precise locations by molecules such as biotin in order to allow attachment to the streptavidin surface. Finally, they are stable to long-term storage. In some cases of chiral compounds, the efficient monitoring of the selection procedure has allowed a very high specificity exemplified by the capability of the aptamer to bind stereoselectively the target. For example, Geiger et al.[26] reported the selection of RNA aptamers that bind L-arginine with submicromolar dissociation constants and high enantioselectivity. Other RNA aptamers have been isolated that can discriminate between L- and D-amino acids although showing relatively poor discrimination factors.[27] Williams et al.[28] produced a stereoselective DNA aptamer. This selected oligonucleotide binds with high affinity the D-enantiomer of an oligopeptide without significant affinity for the L-enantiomer. However, to the best of our knowledge, the enantioselective properties of RNA or DNA aptamers have never been exploited for an application in target-specific chiral separations.

[AVP]
Cys^{1}-Tyr^{2}-Phe^{3}-Gln^{4}-Asn^{5}-Cys^{6}-Pro^{7}-Arg^{8}-Gly^{9}-NH_2

Figure 1. Primary structure of arginine−vasopressin ([AVP]).

The aim of this paper was to examine the feasibility of using a DNA aptamer, characterized by its high enantioselective binding, as a specifically designed chiral selector. A biotinylated DNA aptamer, with stereoselective binding affinity for a test D-peptide (arginine-vasopressin), was immobilized on a streptavidin chromatographic support. The retention and separation of the D- and L-peptides on this novel CSP was investigated in relation to column temperature, pH, and ionic strength of the mobile phase. A mechanism for the chiral discrimination of vasopressin enantiomers was proposed, and the operating conditions for optimal enantiomeric separation were determined.

Experimental Methods

Reagents and Materials. L-Vasopressin (Figure 1) was obtained from Sigma Aldrich (Saint-Quentin, France). D-Vasopressin was synthesized from D-amino acids by Millegen (Toulouse, France) and purified by reversed-phase chromatography (C8 column: 4.6 × 30 mm with a particle diameter of 7 μm; eluent A: H_2O; eluent B: H_2O−acetonitrile 25−75 (v/v); gradient elution by varying the proportion of eluent B in the mobile phase from 2 to 80% in 50 min; flow rate: 1 mL/min; UV detection: 215 nm; injection volume: 100 μL; solute retention time: 13.56 min). The identity of oligopeptide was confirmed by ESI-MS (before cyclization: m/z 1086.6 ($[M + H]^+$); after cyclization: m/z 1084.6 ($[M + H]^+$)). Na_2HPO_4, NaH_2PO_4, KCl, and $MgCl_2$ were supplied by Prolabo (Paris, France). Water was obtained from an Elgastat option water purification system (Odil, Talant, France) fitted with a reverse osmosis cartridge. The 55-base DNA oligonucleotide (Figure 2) was 5′-biotinylated (Eurogentec, Herstal, Belgium).

Biotin phosphoramidite containing a 16-atom spacer arm based on triethylene glycol was used for the aptamer biotinylation. The biotinylated oligonucleotide was purified by gel electrophoresis (Eurogentec). The 2.1 × 30 mm POROS BA column (perfusion chromatography column with 20 μm flow-through particles) and the loading buffer (10 mM phosphate, 150 mM NaCl, pH = 7.2) were obtained from Applied Biosystems (Courtaboeuf, France). In this column, streptavidin was covalently bound to the particle surface.

Stationary Phase Preparation. Prior to immobilization, the biotinylated aptamer was renaturated by heating the oligonucleotide at 70 °C for 5 min in an aqueous buffer (20 mM phosphate buffer, 25 mM

(9) (a) Sellergren, B. *J. Chromatogr. A* **2001**, *906*, 227. (b) Hwang, C. C.; Lee, W. C. *J. Chromatogr. B* **2001**, *765*, 45. (c) Hart, B. R.; Rush, D. J.; Shea, K. J. *J. Am. Chem. Soc.* **2000**, *122*, 460. (d) Mayes, A. G.; Mosbach, K. *Anal. Chem.* **1996**, *68*, 3769. (e) Sellergren, B.; Shea, K. J. *J. Chromatogr. A* **1995**, *690*, 29.

(10) (a) Hofstetter, O.; Lindstrom, H.; Hofstetter, H. *Anal. Chem.* **2002**, *74*, 2119. (b) Nevanen, T. K.; Soderholm, L.; Kukkonen, K.; Suortti, T.; Teerinen, T.; Linder, M.; Soderlund, H.; Teeri, T. T. *J. Chromatogr. A* **2001**, *925*, 89. (c) Hofstetter, O.; Hofstetter, H.; Wilchek, M.; Schurig, V.; Green, B. *Int. J. Bio-Chromatogr.* **2000**, *5*, 165. (d) Hofstetter, O.; Hofstetter, H.; Schurig, V.; Wilchek, M. *J. Am. Chem. Soc.* **1998**, *120*, 3251.

(11) Miyabe, K.; Guiochon, G. *Biotechnol. Prog.* **2000**, *16*, 617.

(12) Jayasena, S. D. *Clin. Chem.* **1999**, *45*, 1628.

(13) Tuerk, C.; Gold, L. *Science* **1990**, *249*, 505.

(14) Ciesiolka, J.; Yarus, M. *RNA* **1996**, *2*, 785.

(15) Ellington, A. D.; Szostak, J. *Nature* **1990**, *346*, 818.

(16) (a) Vianini, E.; Palumbo, M.; Gatto, B. *Biorg. Med. Chem.* **2001**, *9*, 2543. (b) Majerfeld, I.; Yarus, M. *Nat. Struct. Biol.* **1994**, *1*, 287.

(17) (a) Ye, X.; Gorin, A. D.; Ellington, D. A.; Patel, D. J. *Nature Struct. Biol.* **1996**, *3*, 1026. (b) Niewlandt, D.; Wecker, M.; Gold, L. *Biochemistry* **1995**, *34*, 5651.

(18) (a) Golden, M. C.; Collins, B. D.; Willis, M. C.; Koch, T. H. *J. Biotechnol.* **2000**, *81*, 167. (b) Parrott, A. M.; Lago, H.; Adams, C. J.; Ashcroft, A. E.; Stonehouse, N. J.; Stockley, P. G. *Nucleic Acids Res.* **2000**, *28*, 489. (c) Dang, C.; Jayasena, S. D. *J. Mol. Biol.* **1996**, 264, 268. (d) Nazarenko, I. A. Uhlenbeck, O. C. *Biochemistry* **1995**, *34*, 2545.

(19) Kigan, D.; Futamura, Y.; Sakamoto, K.; Yokoyama, S. *Nucleic. Acids Res.* **1998**, *26*, 1755.

(20) (a) Stojanovic, M. N.; de Prada, P.; Landry, D. W. *J. Am. Chem. Soc.* **2001**, *123*, 4928. (b) Zimmermann, G. R.; Jenison, R. D.; Wick, C. L.; Simorre, J. P.; Pardi, A. *Nat. Struct. Biol.* **1997**, *6*, 644. Wallis, M. G.; von Ahsen, U.; Schroeder, R.; Famulok, M. *Chem. Biol.* **1995**, *2*, 543.

(21) Davis, K. A.; Abrams, B.; Lin, Y.; Jayasena, S. D. *Nucleic Acids Res.* **1996**, *24*, 702.

(22) (a) Frauendorf, C.; Jaschke, A. *Bioorg. Med. Chem.* **2001**, *9*, 2521. (b) Jhaveri, S.; Rajendran, M.; Ellington, A. D. *Nat. Biotechnol.* **2000**, *18*, 1293. (c) Potyrailo, R. A.; Conrad, R. C.; Ellington, A. D.; Hieftje, G. M. *Anal. Chem.* **1998**, *70*, 3419.

(23) Drolet, D. W.; Moon-McDermott, L.; Romig, T. S. *Nat. Biotechnol.* **1996**, *14*, 1021.

(24) (a) Pavski, V.; Le, X. C. *Anal. Chem.* **2001**, *73*, 6070. (b) Rehder, M. A.; McGown, L. B. *Electrophoresis* **2001**, *22*, 3759. (c) German, I.; Buchanan, D. D.; Kennedy, R. T. *Anal. Chem.* **1998**, *70*, 4540.

(25) (a) Deng, Q.; German, I.; Buchanan, D.; Kennedy, R. T. *Anal. Chem.* **2001**, *73*, 5415. (b) Romig, T. S.; Bell, C.; Drolet, D. W. *J. Chromatogr. B* **1999**, *731*, 275.

(26) Geiger, A.; Burgstaller, P.; von der Eltz, H.; Roeder, A.; Famulok, M. *Nucleic Acids Res.* **1996**, *24*, 1029.

(27) (a) Famulok, M. *J. Am. Chem. Soc.* **1994**, *116*, 1698. (b) Connell, G. J.; Illangesekare, M.; Yarus, M. *Biochemistry* **1993**, *32*, 5497. (c) Famulok, M.; Szostak, J. W. *J. Am. Chem. Soc.* **1992**, *114*, 3990.

(28) Williams, K. P.; Liu, X. H.; Schumacher, T. N. M.; Lin, H. Y.; Ausiello, D. A.; Kim, P. S.; Bartel, D. P. *Proc. Natl. Acad. Sci. U.S.A.* **1997**, *94*, 11285.

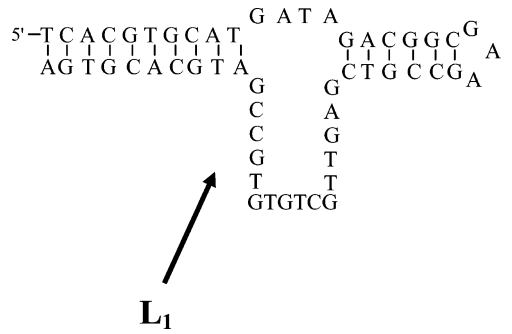

Figure 2. Sequence and secondary structure model of the 55-base DNA aptamer showing the asymmetric internal loop of 20 nucleotides (L_1) which is essential for the specific D-vasopressin enantiomer binding (from ref 28).

KCl, 1.5 mM $MgCl_2$ adjusted to pH 7.6) and left to stand at room temperature for 30 min. The POROS streptavidin column was equilibrated in loading buffer, by washing with ~20 mL. A 29 nmol sample of the modified aptamer was applied to the POROS streptavidin column using a pump fixed at a flow rate of 100 μL/min during 3 h, at room temperature. The column was washed with ~10 mL of loading buffer, and the column washes were added to the unbound DNA solution. The amount of oligonucleotide coupled to the chromatographic support was quantified by subtracting the UV absorbance at 280 nm of the unbound DNA from the initial solutions. When not used, the aptamer column was stored at 4 °C in the loading buffer.

Apparatus. The HPLC system consisted of a LC Shimadzu pump 10AT (Sarreguemines, France), a Shimadzu SIL-10AD auto injector, a Shimadzu SPD-10A UV−visible detector (λ = 195 nm), a Shimadzu SCL-10A system controller with Class-VP software (Shimadzu), and an Igloocil oven (Interchim).

Chromatographic Operating Conditions. The mobile phase consisted of 5 mM phosphate buffer and 3 mM $MgCl_2$. The phosphate buffer was prepared by mixing equimolar solutions of mono- and dibasic sodium phosphate to produce the desired eluent pH. The mobile phase pH ranged from 5.0 to 8.0, the column temperature from 0 to 25 °C, and the eluent KCl concentration from 25 to 100 mM. The mobile phase flow rates (50 or 150 μL/min) were low enough to exclude any split peak effect. To avoid the presence of significant nonlinear effects, the solute amount added onto the column corresponded to the smallest sample size allowing the detection of D-peptide in all operating conditions. Peptide solutions were prepared in the mobile phase at a concentration of 0.9 mM, and 100 nL was injected at least three times.

Determination of the Chromatographic Parameters. The solute retention on the aptamer stationary phase can be evaluated using the retention factor k:

$$k = \frac{t_R - t_0}{t_0} \quad (1)$$

where t_R is the retention time of the solute and t_0 is the column void time. To obtain the thermodynamic retention time, i.e., the accurate measure of solute retention, t_R was determined by calculating the first moment of the peak as previously described.[5a] The void time was determined using the mobile phase peak. The retention times and column void time were corrected for the extracolumn void time. It was assessed by injections of solute onto the chromatographic system when no column was present.

At infinite dilution, i.e., under linear elution conditions, and assuming that nonspecific interactions between solute and chromatographic support were negligible (see below), the retention factor can be related to the association constant between peptide and aptamer K as follows:

$$k = \sigma K \quad (2)$$

where σ is equal to the ratio of the active binding site number in the column (m_L) over the void volume of the chromatographic column (V_M).

The efficiency of the column, reflecting the band broadening, was characterized by estimating the reduced plate height h (the smaller the reduced plate height, the greater the efficiency):

$$h = \frac{L}{d_p N} \quad (3)$$

with

$$N = 5.54\left(\frac{t_R}{\delta}\right)^2 \quad (4)$$

where N is the number of theoretical plates (δ is the peak width at half-height), L is the column length, and d_p is the average particle diameter.

The asymmetry factor A_s, reflecting the peak distortion, was determined by calculating the ratio of the second (or right) part of the peak over the first (or early) part of the peak at 10% of the peak height.

Analysis of the Retention Data. The model equations were fitted to the retention factors of the solutes using the software Table Curve 2D (SPSS Science Software GmbH, Erkrath, Germany).

Results and Discussion

The chromatographic column used in this study consisted of a D-vasopressin-specific DNA aptamer immobilized on a highly porous polystyrene−divinylbenzene support via a biotin−streptavidin bridge. It has been previously established that this 55-base aptamer bound the D-enantiomer of peptide with an association constant of ~1.1 μM^{-1}, while no significant affinity for the L-enantiomer was observed.[28] This aptamer is characterized by an asymmetric internal loop of 20 nucleotides, which is essential for the specific D-vasopressin binding (see Figure 2). A 21 nmol sample of aptamer was immobilized for a bed volume of 100 μL. The maximum binding capacity of the POROS streptavidin media was approximately 12.5 nmol of biotinylated antibody per 100 μL.[29] This difference between oligonucleotide and antibody immobilization indicates that the aptamer can be bound more densely than the antibody due to the difference in the steric effects. Similar conclusions have been drawn by Deng et al.,[25a] who immobilized an adenosine-specific DNA aptamer on a streptavidin support, for the separation of adenosine and analogues by affinity chromatography. The analysis of the enantiomeric mixture was carried out in operating conditions similar to those originally used for the selection of the aptamer.[28] The mobile phase consisted of 5 mM phosphate buffer, 100 mM KCl, and 3.0 mM $MgCl_2$, pH 7.0. The column temperature was set at 20 °C. As shown in Figure 3, the D-peptide was retained by the affinity column, while the L-peptide eluted in the void volume.

This result indicates that the immobilized aptamer binds significantly the D-enantiomer without any significant binding to the L-enantiomer. To explore the mechanistic aspects of this chiral discrimination and to determine the optimal utilization of this aptamer column, experiments were performed under a variety of operating conditions (pH and ionic strength of the mobile phase and column temperature). The chromatographic results are presented below.

Bulk Mobile Phase pH Effects. Vasopressin has three ionizable groups: the N-terminal amino, the arginine guanidine,

(29) As indicated in the operating conditions supplied by Applied Biosystems.

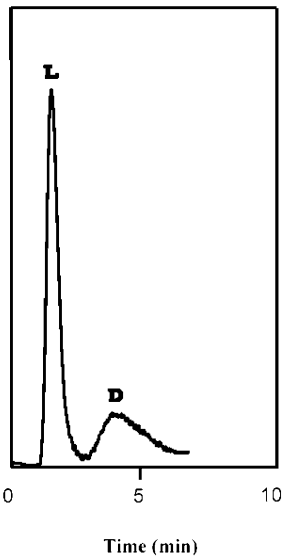

Figure 3. Separation of the vasopressin enantiomer pair (**L**: L-enantiomer; **D**: D-enantiomer) using the target-specific aptamer stationary phase. Column: 2.1 × 30 mm. Temperature: 20 °C. Mobile phase composition: 5 mM phosphate buffer, 100 mM KCl, 3 mM $MgCl_2$, pH 7.0. Flow rate: 150 μL/min. Injection: 100 nL at a concentration of 0.9 mM. UV detection at 195 nm.

and the tyrosine phenol groups. In a peptide, the mean values of pK_a for the arginine guanidine, tyrosine phenol, and cysteine N-terminal amino groups are ~12.5, ~10.5, and ~7.3, respectively.[30] Therefore, at eluent pH values lower than 8.5, arginine guanidine and tyrosine phenol groups are expected to be entirely protonated. On the other hand, the deprotonation of the N-terminal amino group is expected to start at lower eluent pH. By analyzing the pH effects on solute retention in the eluent pH range from 5.0 to 8.0, it was possible to evaluate a possible Coulomb interaction between the peptide N-terminal amino group and phosphate groups of DNA. The column temperature was 20 °C with a mobile phase consisting of 5 mM phosphate buffer, 100 mM KCl, and 3 mM $MgCl_2$. The L-enantiomer eluted in the void volume at all the mobile phase pH's. On the other hand, the D-enantiomer of vasopressin was significantly retained by the column over this eluent pH range. However, no significant variation of k_D was observed over the pH range as presented in Figure 4.

Such retention behavior is consistent with a binding mechanism in which the N-terminal amino group on the D-peptide is not essential to the interaction with the aptamer stationary phase.

Bulk Mobile Phase Salt Effects: The Polyelectrolyte Effect. The knowledge of the salt effect operative in the peptide−DNA interacting system could provide valuable information on the role of the Coulomb interactions in the association process. Previous papers have reported that relations derived from the Wyman concept constitute a valuable tool to describe the salt dependence on the solute retention in hydrophobic, electrostatic interaction and affinity chromatography.[31] The salt effects on the equilibrium constant K between the peptide and the aptamer can be modeled at a thermodynamic

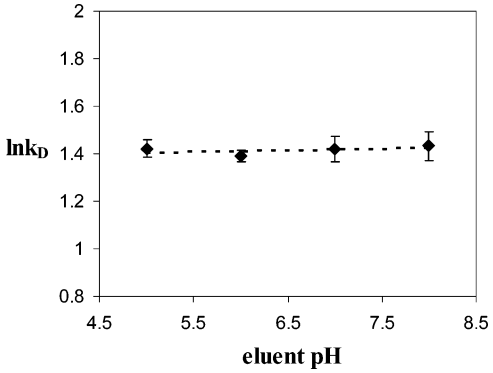

Figure 4. Plot of ln k versus eluent pH for D-peptide (k_D) using the target-specific aptamer stationary phase. pH range: 5.0−8.0. Column: 2.1 × 30 mm. Temperature: 20 °C. Mobile phase composition: 5 mM phosphate buffer, 100 mM KCl, 3 mM $MgCl_2$. Flow rate: 150 μL/min.

level in terms of the direct stoichiometric participation of ions (υ_x) and water (υ_w) in the association reaction. The dependence of K on the mean ionic activity a_x can be formulated as follows, via the linkage Wyman relations modified by Tanford:[32]

$$\frac{\mathrm{d}(\ln K)}{\mathrm{d}(\ln a_x)} = (\Delta\nu_x) - \frac{pm_x}{55.6}(\Delta\nu_w) \qquad (5)$$

where ($\Delta\upsilon_x$) and ($\Delta\upsilon_w$) are respectively the net number of salt ions and water displaced or bound in forming the peptide−DNA complex, m_x is the molal concentration of salt, and p is the total number of ions associated with the electrolyte. At low enough salt concentration, the consequences of water release are insignificant. So, the dependence of K on salt activity provides a measure of the net number of ions released or bound upon complex formation.[33] Assuming that replacing the ionic activity by salt concentration c_x introduces little error over the experimental salt concentration range, an approximate integrated form of the equation is obtained as previously reported:[33]

$$\ln K \cong \ln K_0 + (\Delta\nu_x) \ln c_x \qquad (6)$$

where K_0 is the binding constant in a hypothetical 1 M salt concentration reference state.

Using eqs 6 and 2 the following relation can be obtained:[31a]

$$\ln k \cong \ln k_0 + (\Delta\nu_x) \ln c_x \qquad (7)$$

where k_0 is the retention factor corresponding to K_0.

It is well established that, for the interactions between a cationic ligand and double-stranded or single-stranded DNA, a decrease in the equilibrium association constant is observed with increasing salt concentration.[34] Previous thermodynamic studies have shown that this salt dependence is mainly due to the release of counterions (cations) from the DNA phosphate backbone upon the complex formation.[33,34] The high electrostatic potential from the negatively charged backbone of the nucleic acid is responsible for an accumulation of cations in the vicinity of

(30) Messana, I.; Rosseti, D. V.; Cassiano, L.; Misisti, F.; Giardina, B.; Castagnola, M. *J. Chromatogr. B* **1997**, *699*, 149.
(31) (a) Slama, I.; Ravelet, C.; Grosset, C.; Ravel, A.; Villet, A.; Nicolle, E.; Peyrin, E. *Anal. Chem.* **2002**, *74*, 282. (b) Mazsaroff, I.; Varady, L.; Mouchawar, G. A.; Regnier, F. E. *J. Chromatogr.* **1990**, *499*, 63. (c) Wu, S. L.; Benedek, K.; Karger, B. L. *J. Chromatogr.* **1986**, *359*, 3.
(32) (a) Haroun, M.; Dufresne, C.; Jourdan, E.; Ravel, A.; Grosset, C.; Villet, A.; Peyrin, E. *J. Chromatogr. A* **2002**, *977*, 185. (b) Perkins, T. W.; Mak, D. S.; Root, T. W.; Lightfoot, E. N. *J. Chromatogr. A* **1997**, *766*, 1.
(33) Ha, J. H.; Capp, M. W.; Hohenwalter, M. D.; Baskerville, M.; Record, M. T. *J. Mol. Biol.* **1992**, *228*, 252.
(34) (a) Ackroyd, P. C.; Cleary, J.; Glick, G. D. *Biochemistry* **2001**, *40*, 2911. (b) Mascotti, D. P.; Lohman, T. M. *Biochemistry* **1993**, *32*, 10568. (c) Mascotti, D. P.; Lohman, T. M. *Proc. Natl. Acad. Sci. U.S.A.* **1990**, *87*, 3142. (d) deHaseth, P. L.; Lohman, T. M.; Record, M. T. *Biochemistry* **1977**, *16*, 4783.

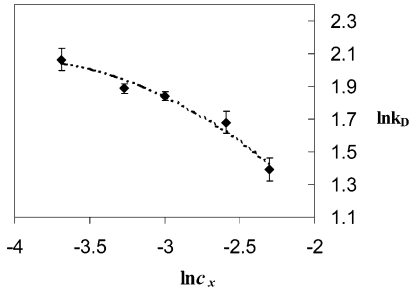

Figure 5. Plot of ln k versus ln c_x for D-peptide (k_D) using the target-specific aptamer stationary phase. KCl concentration (c_x) range: 25−100 mM. Column: 2.1 × 30 mm. Temperature: 20 °C. Mobile phase composition: 5 mM phosphate buffer, 3 mM $MgCl_2$, pH 6.0. Flow rate: 150 μL/min. (- - -) Theoretical curve obtained by fitting eq 9 to the experimental data.

the nucleic acid (polyelectrolyte nature of the nucleic acid). In fact, when a cationic ligand interacts with a nucleic acid, the neutralization of phosphate results in the release of the associated counterions. For the DNA of the length used here (55 bases), DNA behaves as a polyelectrolyte.[35] Therefore, $\Delta\upsilon_x$ can provide an estimate of both the number of DNA phosphate charges neutralized in the interaction and the contribution of the polyelectrolyte effect to the cationic ligand−DNA complex.[33,34] Thus, the following relation can be obtained from eq 7:

$$\ln k \cong \ln k_0 - m'\Psi \ln c_x \tag{8}$$

where m' is the number of ion pairs and Ψ the degree of cation condensation per phosphate (assumed to be 0.76 for single-stranded DNA[34b]). In this approach, the presence of Mg^{2+} as potential competitive cation for phosphate groups has been neglected. Taking into account this effect, the following relation is described:[36]

$$\ln k \cong \ln k_0 - m'\Psi \ln c_x - m' \ln\left[0.5\left(1 + \sqrt{1 + \frac{4K_{Mg}c_{Mg}}{c_x^{2\Psi}}}\right)\right] \tag{9}$$

where c_{Mg} is the Mg^{2+} concentration in the medium and K_{Mg} the equilibrium constant at 1 M between Mg^{2+} and phosphates on DNA.

The analysis of the salt effects was carried out by measuring the retention time of L- and D-peptides in the eluent KCl concentration range from 25 to 100 mM at a column temperature of 20 °C. The mobile phase consisted of 5 mM phosphate buffer and 3 mM $MgCl_2$, pH 6.0. The retention factor of the D-peptide decreased with the mobile phase KCl concentration, while the L-peptide was always eluted in the void volume. Figure 5 shows the ln k versus ln c_x plot for the D-enantiomer at pH 6.0.

To assess if this retention factor change with increasing salt concentration was due to a variation in the binding capacity of the column, the concentration dependencies of the D-peptide retention were measured at different c_x.[37] No change in the number of binding sites was observed when the concentration of salt varied. These results demonstrate that Coulomb interactions participate in retaining the D-peptide. The m' value obtained from eq 9 by a nonlinear regression procedure was 1.0 ± 0.4 ($r^2 = 0.964$), suggesting that only one charge−charge interaction was involved for the D-enantiomer binding.

Column Temperature Effects and Determination of Thermodynamic Parameters. Valuable information about the processes driving the peptide chiral discrimination can be further gained by examining the temperature dependence on solute retention.[38] The temperature dependence of the retention factor is given by the following relation:

$$\ln k = \frac{-\Delta H}{RT} + \frac{\Delta S}{R} + \ln \sigma \tag{10}$$

where ΔH and ΔS are respectively the enthalpy and entropy of transfer of solute from the mobile to the stationary phase, T is the absolute temperature, and R is the gas constant. If the stationary phase, peptide, and solvent properties are independent of temperature and ΔH and ΔS are temperature invariant, a linear van't Hoff plot is obtained. When ΔH and ΔS are temperature dependent, the following logarithmic equation can be given assuming invariance of heat capacity change ΔC_p with temperature:[39]

$$\ln k = \frac{\Delta C_p}{R}\left(\frac{T_H}{T} - \ln\frac{T_S}{T} - 1\right) + \ln \sigma \tag{11}$$

where T_H and T_S are reference temperatures at which ΔH and ΔS are nil. Enthalpy and entropy changes can be evaluated as follows:

$$\Delta H = \Delta C_p(T - T_H) \tag{12}$$

$$\Delta S = \Delta C_p \ln\left(\frac{T}{T_S}\right) \tag{13}$$

The analysis of the thermodynamics was carried out by measuring the D-peptide retention factor in the temperature range from 0 to 25 °C. The mobile phase consisted of 5 mM phosphate buffer and 3 mM $MgCl_2$, pH 6.0. The van't Hoff plot for the D-peptide exhibits a significant nonlinear behavior as shown in Figure 6.

The concentration dependencies of the solute retention factor were also measured at different temperature in order to assess if the nonlinearity of the van't Hoff plot was due to a variation in the number of active binding sites.[37] As reported above for the salt experiments, the binding capacity of the column was

(35) Thompson, M.; Woodbury, N. W. *Biophys. J.* **2001**, *81*, 1793.
(36) Record, M. T.; deHaseth, P. L.; Lohman, T. M. *Biochemistry* **1977**, *16*, 4791.
(37) Under moderate nonlinear conditions, Snyder and co-workers (*J. Chromatogr.* **1987**, *384*, 45) have established that the apparent solute retention factor k_a can be described by the following single function: $k_a = k\int\{[k/(k+1)]N^{1/2}Q_s/m_L\}$ where k and N are respectively the retention factor and the number of theoretical plates (at infinite dilution), m_L is the number of active sites, and Q_s is the amount of solute injected. In two different operating conditions (named 1 and 2) where $[k_1/(k_1+1)]N_1^{1/2} \approx [k_2/(k_2+1)]N_2^{1/2}$, the k_{a1}/k_{a2} ratio is expected to be invariant with Q_s if m_L is constant. Overloading experiments were carried out at the different salt or temperature conditions for which $N_1 \approx N_2$ and $[k_1/(k_1+1)] \approx [k_2/(k_2+1)]$ (for high k values with k_1 not much different from k_2). The k_a ratios were found to be invariant with the amount of solute injected, indicating that no changes in the m_L value occurred with varying salt or temperature.
(38) (a) Miyabe, K. *Anal. Chem.* **2002**, *74*, 2126. (b) Ravelet, C.; Peyrin, E.; Villet, A.; Grosset, C.; Ravel, A.; Alary, A. *Chromatographia* **2001**, *53*, 624. (c) Mozsolits, H.; Lee, T. H.; Wirth, H. J.; Perlmutter, P.; Aguilar, M. I. *Biophys. J.* **1999**, *77*, 1428. (d) Fornstedt, T.; Sajonz, P.; Guiochon, G. *J. Am. Chem. Soc.* **1997**, *119*, 1254. (e) Yashima, E.; Yamamoto, C.; Okamoto, Y. *J. Am. Chem. Soc.* **1996**, *118*, 4036.
(39) Haidacher, D.; Vailaya, A.; Horvath, C. *Proc. Natl. Acad. Sci. U.S.A.* **1996**, *93*, 2290.

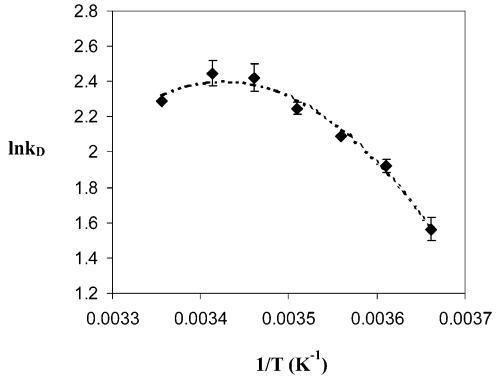

Figure 6. Van't Hoff plot for D-peptide (k_D) using the target-specific aptamer stationary phase. Temperature (T) range: 0−25 °C. Column: 2.1 × 30 mm. Mobile phase composition: 5 mM phosphate buffer, 3 mM $MgCl_2$, pH 6.0. Flow rate: 150 μL/min. (- - -) Theoretical curve obtained by fitting eq 11 to the experimental data.

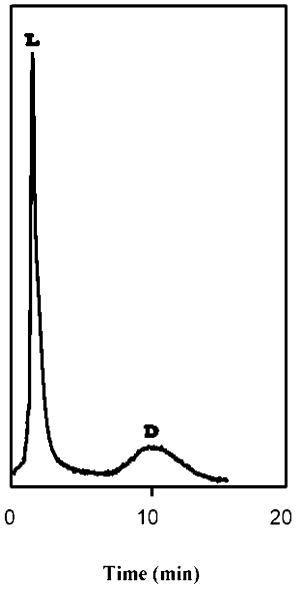

Figure 7. Separation of the vasopressin enantiomer pair (**L**: L-enantiomer; **D**: D-enantiomer) using the target-specific aptamer stationary phase. Column: 2.1 × 30 mm. Temperature: 20 °C. Mobile phase composition: 5 mM phosphate buffer, 3 mM $MgCl_2$, pH 6.0. Flow rate: 150 μL/min. Injection: 100 nL at a concentration of 0.9 mM. UV detection at 195 nm.

invariant when the temperature changed. Therefore, the nonlinearity of the van't Hoff plot is consistent with a large and negative heat capacity change. Figure 7 presents a chromatogram obtained by injection of an enantiomeric mixture at T equal to 20 °C.

From the nonlinear ln k versus 1/T plot, the thermodynamic parameters for D-peptide interaction with the aptamer were determined using eqs 11−13 ($r^2 = 0.983$). Table 1 shows the values of ΔC_p, T_H, T_S, ΔH, and ΔS.

For the determination of T_S and ΔS, the number of moles of immobilized aptamer was used as the m_L value assuming that the aptamer immobilized on the column was available for an interaction with the D-peptide. However, it is not always verified and the number of moles of active binding sites in an affinity protein-based column can be lower than the number of moles of ligand effectively immobilized. This is due to various factors such as steric hindrance, denaturation, or inefficient orientation.[40] For example, it has been shown that from ∼10% to ∼80% of the β-blocker sites,[40a] benzoin sites,[40b] and warfarin sites[40c] are

Table 1. Temperature Dependence of Thermodynamic Quantities Associated with the D-Peptide retention on the Aptamer Stationary Phase As Evaluated by Fitting Eq 11 to Experimental Data[a]

temp (°C)	ΔH (kJ/mol)	ΔS (J/mol·K)	ΔC_p (kJ/mol·K)	T_H (°C)	T_S (°C)
0	71.0 (2.3)	341.0 (10.0)			
4	55.9 (1.2)	286.1 (6.3)			
8	40.8 (0.08)	232.0 (1.6)			
12	25.7 (1.2)	178.6 (2.5)	−3.780 (0.293)	18.8 (0.9)	25.8 (1.4)
16	10.6 (2.4)	126.0 (6.5)			
20	−4.5 (3.5)	74.0 (10.5)			
25	−23.4 (5.0)	10.1 (15.1)			

[a] Standard deviations are in parentheses.

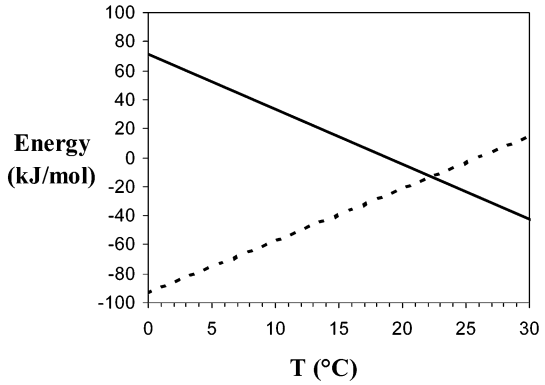

Figure 8. ΔH (—) and $-T\Delta S$ (- - -) plots vs column temperature (T) for D-peptide retention on the target-specific aptamer stationary phase. Column: 2.1 × 30 mm. Mobile phase composition: 5 mM phosphate buffer, 3 mM $MgCl_2$, pH 6.0. Flow rate: 150 μL/min.

active in various protein-based columns. Therefore, T_S and ΔS were also determined using an m_L value arbitrarily fixed to 10 nmol, representing ∼50% of the number of moles of aptamer effectively immobilized. Very low changes in the T_S and ΔS values are observed.[41] For example, at 10 °C, the entropy change was only 3% higher than the ΔS value obtained using the number of moles of ligand effectively immobilized. So, neglecting these effects has no serious consequences on the interpretation of the thermodynamics. As a consequence of heat capacity change, the enthalpic and entropic contributions are strongly a function of temperature. Figure 8 shows the ΔH and $-T\Delta S$ values plotted as a function of the column temperature.

At low temperature, the binding of the D-enantiomer to the aptamer stationary phase is characterized by an unfavorable enthalpy term so that the association process is purely entropically driven. At about 25 °C, the enthalpy change of association was estimated to be approximately −20 kJ/mol with $-T\Delta S$ ∼0 kJ/mol, indicating that the complex formation is enthalpically governed.

Possible Thermodynamic Origins of the D-Peptide Binding to the Immobilized Aptamer. L-Vasopressin does not exhibit any significant retention on the aptamer column under the various operating conditions. This means that possible Coulomb interactions, hydrophobic effects, or van der Waals interactions/hydrogen bonding with the chromatographic support or nonspecific regions of DNA are reduced and can be neglected in

(40) (a) Gotmar, G.; Albareda, R. N.; Fornstedt, T. *Anal. Chem.* **2002**, *74*, 2950. (b) Lloyd, D. K.; Ahmed, A.; Pastore, F. *Electrophoresis* **1997**, *18*, 958. (c) Loun, B.; Hage, D. S. *J. Chromatogr.* **1992**, *579*, 225.
(41) For an m_L value of 10 nmol, T_s was found to be 26.3 °C.

this chromatographic system. Therefore, the D-peptide retention is exclusively dependent on the interactions with the specific binding pocket (the 20-base loop as indicated above). pH experiments suggest that the N-terminal amino group of the D-peptide is not involved in the binding at the stereospecific pocket. Such a behavior can be explained if it is considered that the aptamer has been selected against the target using D-vasopressin linked to the column through its N-terminal amino group. Moreover, no significant difference in the association constants was previously obtained for the D-vasopressin−aptamer or *N*-acetyl D-vasopressin−aptamer complexes.[28] As the salt experiments indicate that one charge−charge interaction occurs in the binding of D-peptide to the aptamer, it is strongly assumed that the arginine guanidine residue engages in a Coulomb interaction with one phosphate group at or near the specific binding loop. This is in agreement with previous data that showed that arginine guanidinium groups are frequently involved in the specific interaction between peptide/protein and nucleic acids. One example of the arginine-rich family of nucleic acid-binding proteins is the tat protein, which interacts specifically with TAR via the binding of a single arginine residue within a bulge situated within an RNA hairpin.[42] Furthermore, a study of Tao and Frankel described an RNA aptamer−arginine complex formation which involved both Coulomb interactions, hydrogen bonding, and stacking interactions.[43] Temperature experiments indicate the presence of a large and negative heat capacity change upon the D-peptide binding (Table 1). A large negative ΔC_p of association is a common feature of site-specific protein−nucleic acid interactions.[44] ΔC_p is classically related to hydration changes between two states of the system. Dehydration of nonpolar groups is a process accompanied by a major negative heat capacity change, while a positive heat capacity change is observed for the dehydration of polar surfaces.[45] Such a large, negative ΔC_p for D-peptide−aptamer interaction is consistent with a complex formation in which several contacts between nonpolar groups of two species are engaged. Consequently, it is strongly assumed that hydrophobic forces play a role in the D-peptide−aptamer complex formation. This effect explains, at least in part (see below), the entropically driven binding process observed at low temperature (Table 1 and Figure 8). However, it is well established that, at 25 °C, the transfer of hydrophobic compounds from water to nonpolar solvents ("pure" hydrophobic effect) is characterized by an enthalpy of formation close to zero and a large, positive entropy contribution.[46] At 25 °C, for the D-peptide−aptamer association, ΔH is approximately −20 kJ/mol (Table 1 and Figure 8). This means that van der Waals interactions and hydrogen bonding (both characterized by negative enthalpy changes at this temperature[46b,47]) are engaged at the complex interface. As $\Delta S \approx 0$ J/mol·K at 25 °C (Table 1 and Figure 8), it appears that there should be some source of negative entropy compensating the large, positive entropy of dehydration. The overall entropy change at 25 °C can be split up in the following way:[45a,47a,48]

$$\Delta S = \Delta S^{\mathrm{dehy}} + \Delta S^{\mathrm{pe}} + \Delta S^{\mathrm{tr/rt}} + \Delta S^{\mathrm{conf}} \approx 0 \qquad (14)$$

where favorable entropic changes include ΔS^{dehy} (entropy change due to dehydration effects) and ΔS^{pe} (entropy change due to the polyelectrolyte effect) and unfavorable contributions include $\Delta S^{\mathrm{tr/rt}}$ (entropy change associated with the loss of translational and rotational degrees of freedom) and ΔS^{conf} (entropy change due to the loss of conformational freedom). The positive entropy contribution from counterion removal (polyelectrolyte effect) is estimated to be weak (20 J/mol·K).[49] In addition, direct experimental studies have shown that the entropy cost due to the reduction of translational and rotational degrees of freedom is small, i.e., $\Delta S^{\mathrm{tr/rt}}$ is about −20 J/mol·K.[50] So, the major negative contribution to the entropy change would result mainly from the conformational entropy contribution, and an estimate of ΔS^{conf} can be obtained as follows:

$$\Delta S^{\mathrm{conf}} \approx -\Delta S^{\mathrm{dehy}} = -(\Delta S_{\mathrm{np}}{}^{\mathrm{dehy}} + \Delta S_{\mathrm{p}}{}^{\mathrm{dehy}}) \qquad (15)$$

where entropic effects of dehydration can result from the water release from both nonpolar ($\Delta S_{\mathrm{np}}{}^{\mathrm{dehy}}$) and polar ($\Delta S_{\mathrm{p}}{}^{\mathrm{dehy}}$) groups at the interface.[47a] Using the quantitative relationships previously developed for the analysis of various protein−DNA association thermodynamics, $\Delta S_{\mathrm{np}}{}^{\mathrm{dehy}}$ was estimated to be ∼1300 J/mol·K at 25 °C.[51] Although $\Delta S_{\mathrm{p}}{}^{\mathrm{dehy}}$ cannot be evaluated, the polar group dehydration can only increase the positive component of the association entropy.[47a] Therefore, ΔS^{conf} is lower than −1300 J/mol·K. This unfavorable conformational entropy change could proceed from fixation of side chains at the interface and structural changes in the interacting molecules upon complex formation. The conformational entropy of fixing an average amino acid residue is about −40 J/mol·K.[45a,47a] So, the maximal entropy cost for the D-peptide binding is ca. −360 J/mol·K. This means that an other major negative entropy component comes from some structural changes in the interacting molecules upon complex formation. This expected behavior squares with the general feature of the association between peptide/protein and nucleic acid aptamer. Adaptive conformational transitions are classically associated with complex formation where both components are able to adjust their recognition surfaces in order to maximize complementarity through tightly packed contacts involving stacking, Coulomb interactions, and hydrogen bonding.[52]

Chromatographic Properties of the Target-Specific Aptamer Column. Enantioselectivity and Analysis Time. The main advantage of the target-specific aptamer column is that the enantioselectivity is very significant since the stationary phase binds only to the D-enantiomer; that is, the L-peptide interaction with the stationary phase is negligible whatever the operating conditions investigated. The separation factor is higher than the one classically observed with the imprinted chiral selectors[9a] and in the same order of magnitude as the one obtained using

(42) (a) Tao, J.; Frankel, A. D. *Proc. Natl. Acad. Sci. U.S.A.* **1992**, *89*, 2723. (b) Calnan, B. J.; Tidor, B.; Biancalana, S.; Hudson, D.; Frankel, A. D. *Science* **1991**, *252*, 1167.
(43) Tao, J.; Frankel, A. D. *Biochemistry* **1996**, *35*, 2229.
(44) Ha, J. H.; Spolar, R. S.; Record, M. T. *J. Mol. Biol.* **1989**, *209*, 801.
(45) (a) Liggins, J. R.; Privalov, P. L. *Proteins* **2000**, *4*, 50. (b) Srisvastava, D. K.; Wang, S.; Peterson, K. L. *Biochemistry* **1997**, *36*, 6359.
(46) (a) Baldwin, R. L. *Proc. Natl. Acad. Sci. U.S.A.* **1986**, *83*, 8069. (b) Ross, P. D.; Subramanian, S. *Biochemistry* **1981**, *20*, 3096.
(47) (a) Privalov, P. L.; Jelesarov, I.; Read, C. M.; Dragan, A. I.; Crane-Robinson, C. *J. Mol. Biol.* **1999**, *294*, 997. (b) Jelesarov, I.; Bosshard, H. R. *J. Mol. Recognit.* **1999**, *12*, 3.
(48) Spolar, R. S.; Record, M. T. *Science* **1994**, *263*, 777.
(49) ΔS^{pe} was evaluated considering that the free energy contribution is primarily entropic, as proposed in ref 48.
(50) Tamura, A.; Privalov, P. L. *J. Mol. Biol.* **1997**, *273*, 1048.
(51) $\Delta S_{\mathrm{np}}{}^{\mathrm{dehy}}(T) = 1.35\Delta C_p \ln(T/386)$ from ref 48.
(52) (a) Hermann, T.; Patel, D. J. *Science* **2000**, *287*, 820. (b) Patel, D. J. *Curr. Opin. Chem. Biol.* **1997**, *1*, 32.

stereoselective monoclonal antibodies[10a] (for which the interaction of the nontarget enantiomer with immobilized antibody is also negligible). Here, it can be noted that the aptamer immobilization could affect the binding properties of the selector. However, such a possible behavior is expected to have a reduced effect since the chiral discrimination properties of the aptamer are maintained upon immobilization. So, the immobilization effects via streptavidin−biotin reaction allow the conservation of the stereoselective properties of DNA, and such an attachment procedure is useful for HPLC application. Both the separation of the vasopressin enantiomers and the analysis time can be easily modulated by varying the mobile phase salt concentration and the column temperature. Peptide enantiomers cannot be completely resolved using a high ionic strength mobile phase at a low column temperature. Baseline separation in a short time (around 7 min) is achieved at ambient temperature with 100 mM KCl in the mobile phase (Figure 3) or at a lower temperature without KCl in the eluent. At ambient temperature, a significant enhancement of the enantioselectivity, associated with a concomitant increase in the analysis time (around 15 min), is obtained when a low ionic strength mobile phase is used (Figure 7).

Band Broadening and Peak Asymmetry. Using eqs 3 and 4, the reduced plate height of the D-enantiomer was estimated to be comprised between 35 and 40 at a flow rate of 150 μL/min. As a comparison, the reduced plate height observed for L-phenylalanine anilide (the more retained enantiomer) on an imprinted chiral stationary phase varied from 35 to 150 with flow rate increasing.[9e] On the antibody-based chiral stationary phase, the *h* values obtained for the more retained enantiomer of various amino acids were comprised between 20 and more than 200 in relation to the flow rate and the compound type.[53] In addition, the D-peptide peak distortion was reflected by an asymmetry factor around 1.5 (ideal A_s is 1). When only one type of site is involved in the solute binding to the stationary phase as expected for the immobilized aptamer, broad and unsymmetrical peaks are the consequence of slow mass transfer kinetics (homogeneous kinetics tailing).[54] Several recent studies have demonstrated that target−aptamer complex formations are characterized by small rate constants,[55] as expected for a two-step association process that includes a rapid bimolecular association followed by rate-limiting slow structural changes which mediate the binding surface complementarity.[55c] So, no doubt that slow association−dissociation kinetics contribute significantly to the peak broadening and asymmetry that are observed with the aptamer column. Efficiency as well as peak shape can be significantly improved by increasing the Stanton number.[54] For example, the *h* value for the D-enantiomer was around 15 and $A_s \approx 1.2$ at a lower flow rate of 50 μL/min.

Column Stability. The column stability was evaluated by comparing the D-peptide retention factor before and after more than five months in the same conditions. No significant change in retention time was observed. This demonstrates the stability of the aptamer column during an extended period of time.

Concluding Remarks

In this paper, we report for the first time the use of an immobilized DNA aptamer as a new target-specific chiral stationary phase for high-performance liquid chromatography. Immobilized DNA aptamers could soon become very attractive chiral stationary phases specifically designed against an enantiomer since experiments show high stereospecificity, valuable binding capacity, and stability during an extended period of time. In addition, this work shows that an aptamer immobilized on a chromatographic support constitutes a valuable tool for examining the mechanistic aspects of the target−DNA complex formation. More overall, this new type of chiral selector could find applications in various other fields of chemistry such as enantioselective solid phase extraction, binding assays, and sensors. Further experiments are now in progress in our laboratory in order to select a stereoselective DNA aptamer against other enantiomeric compounds such as amino acids.

Acknowledgment. This work was supported by the Fonds National de la Science (ACI program "nouvelles méthodologies analytiques et capteurs").

JA034483T

(53) *h* was calculated from the chromatographic data presented in ref 10a.

(54) (a) Gotmar, G.; Fornstedt, T.; Guiochon, G. *J. Chromatogr. A* **1999**, *831*, 17. (b) Fornstedt, T.; Zhong, G.; Guiochon, G. *J. Chromatogr. A* **1996**, *742*, 55. (c) Fornstedt, T.; Zhong, G.; Guiochon, G. *J. Chromatogr. A* **1996**, *741*, 1.

(55) (a) Liss, M.; Petersen, B.; Wolf, H.; Prohaska, E. *Anal. Chem.* **2002**, *74*, 4488. (b) Berezovski, M.; Krylov, S. N. *J. Am. Chem. Soc.* **2002**, *124*, 13674. (c) Beckingham, J. A.; Glick, G. D. *Biorg. Med. Chem.* **2001**, *9*, 2243. (d) Gebhardt, K.; Shokraei, A.; Babaie, E.; Lindqvist, B. H. *Biochemistry* **2000**, *39*, 7255.